LL

KEK Preprint 95-176
December 1995
A

Characteristics of the Results of Measurement on 1.3 GHz High Gradient Superconducting Cavities

E. KAKO, S. NOGUCHI, M. ONO, K. SAITO, T. SHISHIDO, T. FUJINO,
Y. FUNAHASHI, H. INOUE, M. MATSUOKA, T. HIGUCHI,
T. SUZUKI and H. UMEZAWA

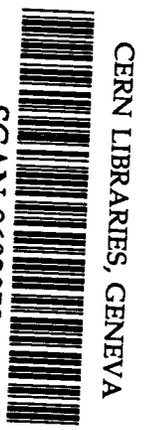

SW96-11

Submitted to the 7th Workshop on RF Superconductivity,
CEA-Saclay, Gif-sur-Yvettte, France, October 17 - 20, 1995.

National Laboratory for High Energy Physics, 1995

KEK Reports are available from:

Technical Information & Library
National Laboratory for High Energy Physics
1-1 Oho, Tsukuba-shi
Ibaraki-ken, 305
JAPAN

Phone: 0298-64-5136
Telex: 3652-534 (Domestic)
(0)3652-534 (International)
Fax: 0298-64-4604
Cable: KEK OHO
E-mail: Library@kekvax.kek.jp (Internet Address)

Characteristics of the Results of Measurement on 1.3 GHz High Gradient Superconducting Cavities

E. Kako, S. Noguchi, M. Ono, K. Saito, T. Shishido, T. Fujino, Y. Funahashi, H. Inoue, M. Matsuoka*, T. Higuchi**, T. Suzuki** and H. Umezawa***

KEK, National Laboratory for High Energy Physics
1-1 Oho, Tsukuba-shi, Ibaraki-ken, 305 Japan

Abstract

Single-cell cavities were made from different niobium materials, which have an RRR (residual resistivity ratio) of 100, 200 and 350. These cavities were prepared by a similar surface treatment: heavy first polishing of more than 160 μm, heat treatment at 760°C or 1400°C, and high pressure water rinsing with a pressure of 85 kg/cm^2. The maximum accelerating gradients of more than 25 MV/m have been reproducibly achieved in the cavities made from both RRR = 200 and RRR = 350. No significant difference in the quench fields that depends on the temperature of heat treatment was observed.

1. Introduction

In superconducting cavities, thermal quench and field emission are the main obstacles limiting the maximum accelerating gradient (Eacc,max). Efforts to achieve a higher accelerating gradient have been made in many laboratories, and a steady progress in understanding these phenomena has been achieved in the past decade. About 15 years ago, the importance of a thermal conductivity in niobium was predicted by a thermal model on a quench field [1]. The calculations in this model showed that the quench field was dependent on the size and resistance of the defects as well as the thermal conductivity of niobium. The effectiveness of a high RRR material was confirmed in the experiments on the x-band cavities with RRR between 25 to 1400 [2]. Therefore, development of a high RRR niobium with a high thermal conductivity is continuing as an essential factor in achieving a higher accelerating gradient. In addition, effective methods to suppress field emission have also been developed. The influence of heat treatment above 1100°C on field emission was investigated in 1.5 GHz cavities at Cornell [3], and the experiment showed that heat treatment was effective in increasing the Eacc,max limited by field emission. High power pulsed rf processing (HPP) was shown to be an effective means of reducing field emission loading in 3 GHz cavities at Cornell [4]. HPP was established as an *in-situ* procedure to recover a degraded cavity performance. Recently, an onset field of field emission has been markedly increased by an improved clean environment and by development of high pressure water rinsing (HPR). HPR was used as a final cleaning step in 1.5 GHz cavities at CEBAF; E_{peak} of 50 MV/m were reproducibly achieved without field emission [5].

In the experiments described above, systematic cavity tests were required to clear their effectiveness in achieving a high accelerating gradient. Since cavity performances are governed by many factors, the reproducibility and statistics of the test results are very important in discussing these performances.

Thirty tests on eight cavities were carried out at KEK. These cavities were prepared by the standard surface preparation procedure established for the TRISTAN superconducting cavities [6], and HPR in addition. As removal thickness of the cavity surface is one of the important factors which determine the cavity performance [7], a sufficient surface removal was carried out to eliminate this influence. The attainable Eacc,max with this surface preparation and the cause of the limitation were investigated with regard to the niobium materials and the temperature of heat treatment. In this paper, an RRR dependence of the obtained Eacc,max and residual surface resistance is shown, and the necessity of high purity niobium materials is discussed. The observations of thermal quench phenomena at high fields are also reported.

2. Cavity and Surface Treatment

Eight cavities were prepared for this experiment. These cavities were made from different niobium materials as summarized in Table I. They are classified by an initial RRR of the niobium sheet and a temperature of heat treatment. These cavities were fabricated at CEBAF, MHI and KEK.

The main cavity parameters calculated by SUPER-

Table I. Summary of the cavities.

cavity	niobium sheet RRR	t [mm]	maker	fabrication forming/EBW	heat treatment
MK-0	100	2.5	Heraeus	MHI/KEK	760°C, 5h
M-3	200	2.0	Tokyo Denkai	MHI	760°C, 5h
M-4	200	2.5	Tokyo Denkai	MHI	760°C, 5h
K-3	200	2.5	Tokyo Denkai	KEK	760°C, 5h
C-3	350	3.2	Fansteel	CEBAF	760°C, 5h
M-1	100	2.5	Heraeus	MHI	1400°C, 4h
K-1	200	2.5	Tokyo Denkai	KEK	1400°C, 6h
C-1	350	3.2	Fansteel	CEBAF	1400°C, 6h

* MHI, Mitsubishi Heavy Industries Ltd.
** Nomura Plating Co., Ltd.
*** Tokyo Denkai Co., Ltd.

Table II. Summary of cavity parameters.

cavity		M-1, MK-0 M-3, M-4	K-1 K-3	C-1 C-3
R/Q	[Ω]	110	101	102
G	[Ω]	266	269	274
Esp/Eacc	[-]	1.89	1.83	1.78
Hsp/Eacc	[Oe/MV/m]	43.2	45.2	43.8

FISH are summarized in Table II. The slight difference in the parameters for each cavity arises from the different cell shape and diameter of the beam tube [8]. The ratio of Esp/Eacc for a single-cell cavity is a relatively low value in comparison with that of a multi-cell cavity.

Every cavity was prepared by a similar surface treatment. The standard surface preparation procedure is summarized as follows. In the first polishing, a surface removal of 160 ~ 300 μm was usually carried out by electro-polishing, EP. EP is suitable for heavy polishing because the chemical reaction is controlled by an applied current. The surface roughness, Rz, of 0.5 μm and the removal speed of 0.6 μm/min at 30°C were obtained. Tumbling (barrel polishing [9]) of about 50 μm was carried out before EP in the cavities with an injured surface: M-1, MK-0, K-3 and C-3.

Heat treatment at 760°C was carried out for hydrogen degassing to avoid Q-disease. The heat treatment was performed for 5 hours at the vacuum pressure of 10. - 3.5 x 10^{-6} Torr. Heat treatment at 1400°C for 6 hours was carried out with titanium gettering for purification. The vacuum pressure at 1400°C was 10. - 3. x 10^{-6} Torr. The RRR was measured with niobium samples, which were treated together with the cavity. The RRR did not change after heat treatment at 760°C and increased by a factor of 1.2 ~ 1.8 after heat treatment at 1400°C [10].

In the final polishing, 10 ~ 50 μm was removed by chemical polishing, CP. The surface roughness was 3 μm, and the removal speed was 10 μm/min at 25°C.

A similar surface removal was carried out in the following test to confirm the reproducibility of the results. After CP, careful shower rinsing with ultrapure water was carried out for 10 minutes in a clean booth. Then, HPR with a pressure of 85 kg/cm^2 was performed for 60 minutes, and 700 liters of ultrapure water was used during this process. Finally, over-flow rinsing combined with ultrasonic agitation was carried out in a hot bath for 60 minutes. The cavity was filled with filtered nitrogen gas while the water inside the cavity was dumped. (Chemical treatment and rinsing were carried out at a company, and it took about 2 hours to transport the cavity to KEK.)

The cavity was assembled in a class 10 clean room, and the wet cavity was immediately pumped out. Baking at 80°C was carried out for 1 night. Prior to a vertical cold test, pre-cooling by liquid nitrogen was carried out for 1 night to save consumption of liquid helium. The vacuum pressure in the cavity was usually 1. x 10^{-9} Torr at room temperature and 5. x 10^{-10} Torr at low temperature.

3. Results and Discussions

3 - 1. Maximum accelerating gradient (Eacc,max)

The obtained Eacc,max in each cavity test is shown in Fig. 1. The limiting factors of the Eacc,max are classified in terms of thermal quench and field emission (rf power). In this figure, thermal quench induced by field emitted electrons is indicated by both symbols superimposed. Field emission was identified by the following diagnostics; electron currents picked up by a probe, x-ray emission detected by PIN photo-diodes, a mapping pattern of temperature rises and an exponential drop of Q_0 values. Strong field emission at less than 25 MV/m was observed in four cavity tests, but reappearance in the same cavity was scarce. In the cavities made from the RRR = 100 material, MK-0 and M-1, the Eacc,max were limited to relatively low fields by thermal quench. These quench fields did not improve in the successive tests after an additional surface removal of 50 μm. In these cavities, abnormal heating spots on the EBW seam at the equator were observed during

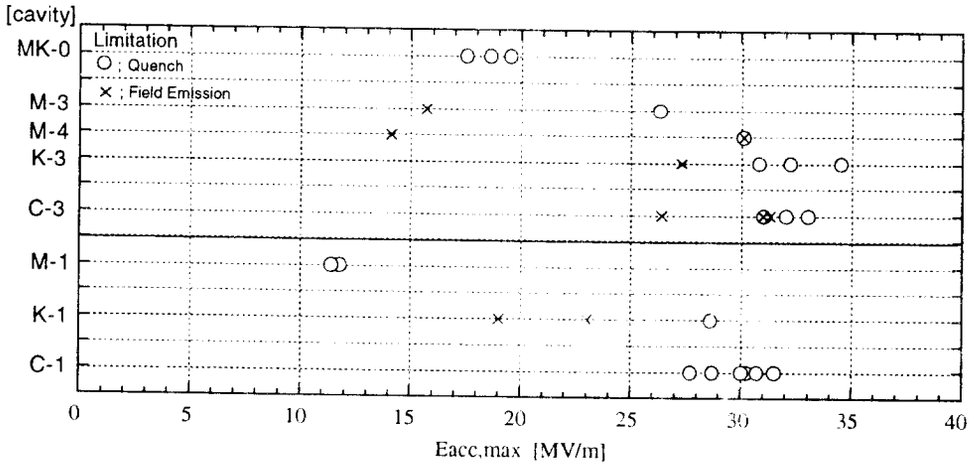

Fig. 1 Summary of the obtained Eacc,max in each cavity

thermal quench. On the other hand, the quench fields above 25 MV/m were obtained in the cavities made from both niobium materials of RRR = 200 and RRR = 350. These quench fields are also reproducible in the repeated cavity tests.

Typical Q_0 - Eacc plots in the eight cavities are shown in Fig. 2. The Eacc,max in each test was limited by thermal quench, and self-pulsing (a periodical thermal quench phenomenon) was usually observed at the Eacc,max. Processing levels at around 20 MV/m due to multipacting were observed in some cavities, and this was processed out by short cw rf processing. The Q_0 values in the M-3 and M-4 cavities were considerably low in comparison with others. This was due to an installation of the temperature mapping system, and this effect is discussed in the next section.

The quench field at 1.8 K as a function of RRR is shown in Fig. 3. The value of RRR is the initial value before heat treatment in order to determine the effect of the temperature of heat treatment. No significant difference in the quench fields has been observed between RRR = 200 and RRR = 350. The quench fields have not been improved even after heat treatment at 1400°C. The results for the cavities with an RRR of more than 200 is summarized as follows ; The thermal quench occurs at around 30 MV/m, and the quench fields are not dependent on the RRR.

3 - 2. Thermal Quench Phenomenon

Thermal quench arises in rapid transition from a superconducting state to a normal conducting state. The energy stored in the cavity is dissipated at the normal conducting area in an instant. This phenomenon is observed by the decay of the accelerating gradient. The time constant, τ-q, as a function of the quench field is shown in Fig. 4. The time constant is defined as the decay time, which the accelerating gradient at quench was decreased to half. The time constant shortened with higher quench fields (larger stored energy), and it was about 200 μsec at 30 MV/m (14 Joule). It is suspected that this effect is related to the spreading speed of the normal conducting area during thermal quench.

The temperature dependence of the quench field was investigated at 1.8 ~ 4.2 K and is shown in Fig. 5. The thermal quench at 1.8 K occurred at 31 MV/m. However, just at the λ-point (2.17 K), the quench field drastically dropped to around 20 MV/m. This drop is considered to be due to the difference in cooling mechanisms between He-II (superfluid) and He-I (nucleate boiling). An interesting phenomenon was

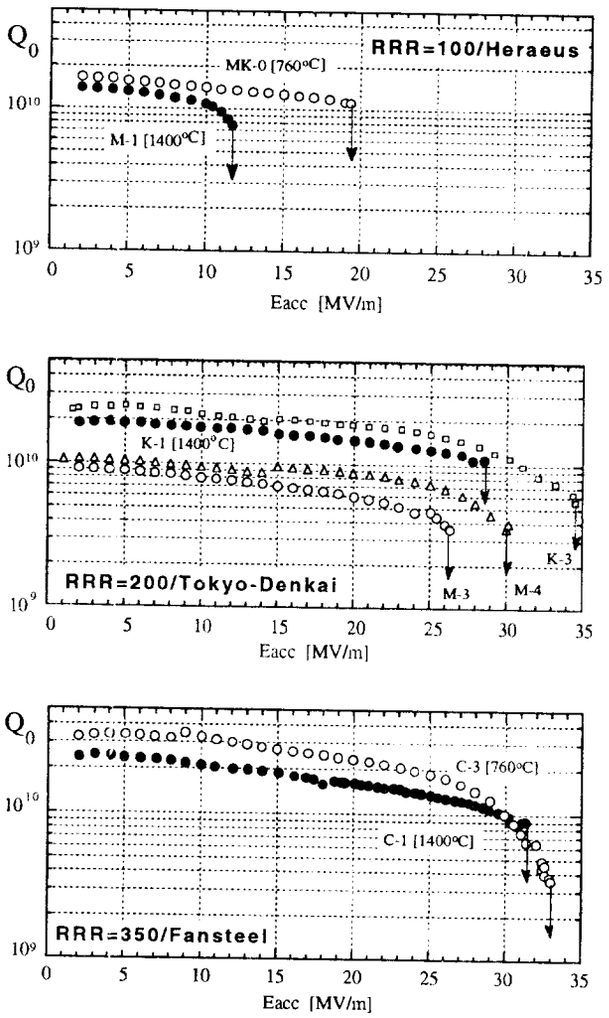

Fig. 2 Q_0 - Eacc plots in the cavities made from a niobium material with each RRR.

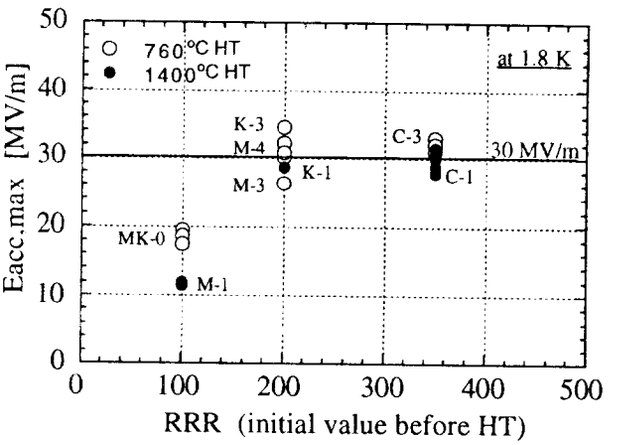

Fig. 3 RRR dependence of the Eacc,max limited by a thermal quench at 1.8 K.

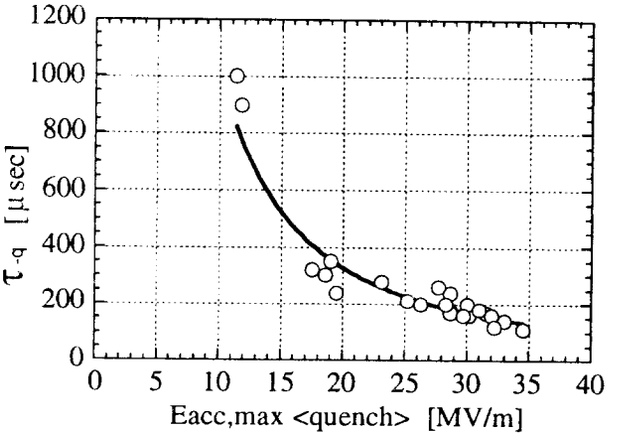

Fig. 4 Time constants (τ-q) as a function of the quench field at 1.8 K.

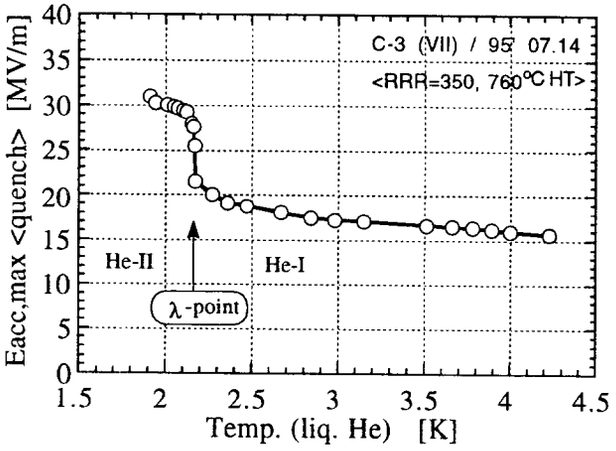

Fig. 5 Temperature dependence of the quench field.

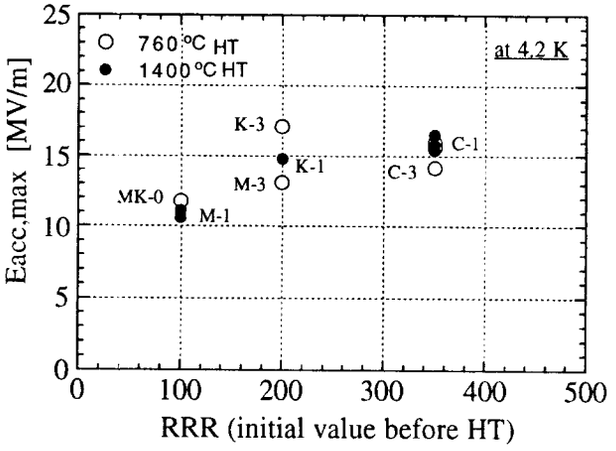

Fig. 6 RRR dependence of the Eacc,max limited by a thermal quench at 4.2 K.

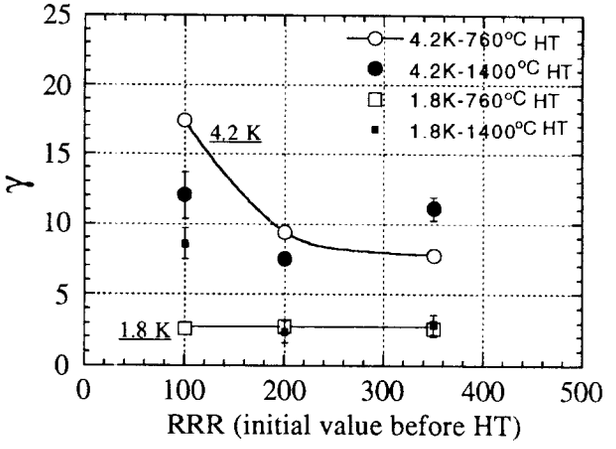

Fig. 7 A correlation with γ and RRR.

observed by thermometry. Thermal quenches originated at the different locations for the temperatures: 1.8 K, 2.6 K and 4.2 K. The thermal quench at these temperatures seems to depend on a critical condition of thermal balance among heat production, thermal conductivity in niobium, surface conditions at the boundary of Nb/He and a bath temperature. Reducing the temperature to 1.5 K, an increase of quench field up to 35 MV/m is expected in extrapolation of the results in Fig. 5. The widest normal conducting area at thermal quench was observed at just below the λ-point, and the spread was more than one third of the whole cavity.

The quench field at 4.2 K as a function of RRR is shown in Fig. 6. The quench fields at 4.2 K in the RRR = 100 cavities were lower than others, similar to the results at 1.8 K. An rf loss by a surface current at 15 MV/m is estimated to be 0.2 W/cm^2 around the equator. This value is very close to the nucleate boiling limit in helium at 4.2 K [11]. Therefore, these quench fields might show a limitation under helium cooling at 4.2 K, though this value is strongly dependent on the conditions of the outer surface in the cavity.

The Q_0 values are gradually degraded with increasing accelerating gradients, (see Fig. 2). A linear increase of the surface resistance, Rs, with the square of the surface electric field, Esp, is obtained in the $1/Q_0$ - Esp^2 plot if no field emission loading. The value of γ is defined by the slope in this plot and is given by the following equation [12];

$$\Delta Rs / Rs = Q_0 (\Delta 1/Q_0) = \gamma (Hsp / H_C)^2.$$

It is believed that the increment of Rs is caused by the temperature rise at an rf surface, thus the information of the thermal conductivity in niobium is contained in the value of γ. A correlation with γ and RRR is shown in Fig. 7. The value of γ was obtained at the Eacc of 8 ~ 12 MV/m. At 4.2 K, γ decreases with RRR, and this trend is very similar to the correlation of a reciprocal of the thermal conductivity with RRR. On the other hand, γ is nearly constant at 1.8 K for all the results except one. This result suggests that the thermal conductivity at 1.8 K might not be so different in each RRR cavity. This idea is consistent with the results of the quench field at 1.8 K.

3 - 3. Residual Surface Resistance (Rres)

The temperature dependence of the surface resistance, Rs(T), at a low field was measured during cooling down from 4.2 K to 1.8 K. BCS surface resistance, $R_{BCS}(T)$, and Rres are obtained by fitting the data of Rs(T). The average value of R_{BCS} (T) in the experiments of 30 cavity tests was obtained as follows;

$$R_{BCS} (T) = 1.50 \times 10^{-4} / T \exp [- 18.3 / T].$$

Where, R_{BCS} (1.8K) = 3.2 ± 0.4 nΩ, and R_{BCS} (4.2K) = 460 ± 70 nΩ. No clear difference between the niobium materials was observed beyond this error.

The RRR dependence of Rres is shown in Fig. 8. The sign of X indicates the cavity tests with an installation of the temperature mapping system. The rf losses at the end plate made from stainless steel is estimated to be less than 0.5 nΩ by SUPERFISH, and the residual magnetic field of 15 mGauss exists inside the cryostat. Therefore, the main part of Rres is considered to be the influence of the residual magnetic field. Additional losses (R_H) due to the residual magnetic field, H_{ext}, is given by the following equation [13],

$$R_H = (\omega \mu_0 \rho_n / 2. RRR)^{1/2} H_{ext} / H_{C2}.$$

Where, H_{C2} is the upper critical field of niobium, and ρ_n is the normal resistance of niobium at room temperature. Therefore, Rres due to the residual magnetic field is in proportion to $1/(RRR)^{1/2}$, and Rres

has a smaller value in a higher RRR niobium material as observed in Fig. 8. The temperature mapping system had magnetized components, about 700 springs made from iron. The influence of the magnetic field in Rres was enhanced by the installation of the temperature mapping system. The difference in Rres between presence and absence of the temperature mapping system, ΔRres*, has a clear dependence on $1/(RRR)^{1/2}$ as shown in Fig. 9.

In the cavities after heat treatment at 1400°C, Rres was relatively larger than that at 760°C. It is supposed that the mechanism of trapping the residual magnetic field might be dependent on grain sizes and grain boundaries in niobium.

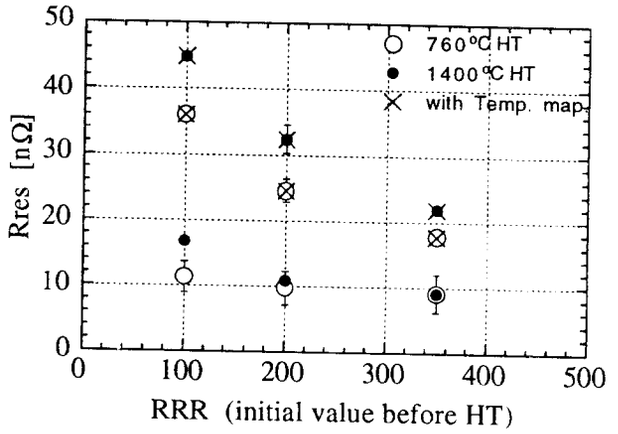

Fig. 8 RRR dependence of the residual surface resistance (Rres).

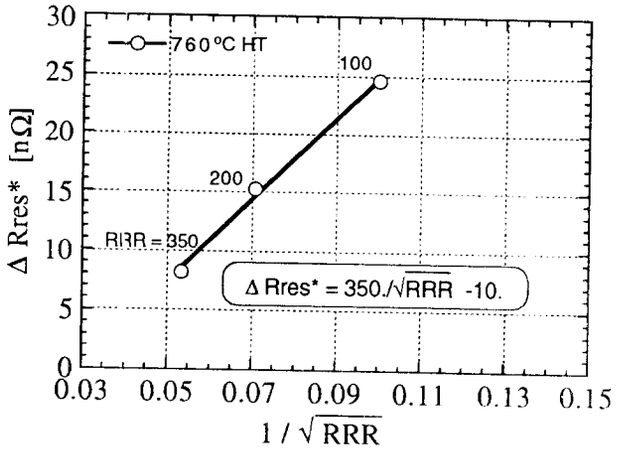

Fig. 9 RRR dependence of the increment of the residual surface resistance (ΔRres*) due to the installation of the temperature mapping system.

4. Conclusions

In the surface preparation at KEK, the possibility of field emission at less than 25 MV/m was drastically decreased. As a result, it was revealed that the thermal quench at around 30 MV/m was the limiting factor of the Eacc,max in this experiment. However, the effectiveness of high RRR materials and heat treatment at 1400°C was not observed in the obtained quench fields in contrast to the previous reports. These results question the necessity of high purity niobium materials like RRR of more than 500, [14].

The obtained quench fields at 1.8 K were lower than the theoretical value calculated for a defect free surface. Understanding the mechanism of the thermal quench phenomena at these fields is essential in the achievement of a further high accelerating gradient.

Acknowledgments

The authors are indebted to Profs. Y. Kimura, K. Takata, S. Kurokawa and Y. Yamazaki for their continuing support and encouragement. Special thanks are given to Dr. K. Hosoyama and Mr. Y. Kojima for their cooperation in supplying liquid helium. One of us, E. Kako, would like to thank Dr. M. Wake for many fruitful discussions about the nature of liquid helium.

References

[1] H. Padamsee, "Calculations for Breakdown Induced by Large Defects in Superconducting Niobium Cavities", IEEE Trans. Mag-19 (1983) P1322-1325.

[2] H. Padamsee, "Influence of Thermal Conductivity on the Breakdown Field of Niobium Cavities", IEEE Trans. Mag-21 (1985) P149-152.

[3] Q.S. Shu, et. al., "A Study of the Influence of Heat Treatment on Field Emission in Superconducting RF Cavities", Nucl. Instr. & Meth., A278 (1989), p329-338.

[4] J. Graber, et. al., "Reduction of Field Emission in Superconducting Cavities with High Power Pulsed RF", Nucl. Instr. & Meth., A350 (1994), p572-581.

[5] P. Kneisel, et. al., "Experience with High Pressure Ultrapure Water Rinsing of Niobium Cavities", Proc. of the 6th SRF workshop, CEBAF (1993) p628-636.

[6] K. Saito, et. al., "R & D of Superconducting Cavities at KEK", Proc. of the 4th SRF workshop, KEK (1989) p635-694.

[7] P. Kneisel, (private communications).

[8] E. Kako, et. al., "Test Results on High Gradient L-band Superconducting Cavities", Proc. of the 6th SRF workshop, CEBAF (1993) p918-943.

[9] T. Higuchi, et. al., "Investigation on Barrel Polishing for Superconducting Niobium Cavities", in this workshop.

[10] K. Saito, et. al., "TESLA Activities at KEK", Proc. of the 6th SRF workshop, CEBAF (1993) p372-381.

[11] H. Safa, (private communications).

[12] S. Noguchi, et. al., "Measurement of a Superconducting 500 MHz Nb Cavity in the TM_{010}-Mode", Nucl. Instr. & Meth., 179 (1981), p205-215.

[13] P. Kneisel and B. Lewis, "Additional RF - Surface Resistance in Superconducting Niobium Cavities Caused by Trapped Magnetic Flux", CEBAF-Technical Note, TN # 94-028 (1994).

[14] J. Graber, "High Gradient Superconducting RF Systems", IEEE Part. Acc. Conf., Dallas (1995), to be published. CLNS - 95 / 1337.

Appendix I. Summary of the surface treatments and the test results.

cavity	RRR	test	heat treatment [°C]	surface treatment [μm]	Eacc,max [MV/m]	Rres [nΩ]	limitation
MK-0	100			Tum.(-), EP-240			
		I	760	CP-25, HPR	19.5	13.8	quench
		II		CP-50, HPR	18.6	36.0 *	quench
		III	760	HPR"	17.5	9.0	quench
M-3	200			EP-160			
		I	760	CP-20, HPR	15.7	7.2	field emission
		II		CP-50, HPR	26.3	26.4 *	quench
M-4	200			EP-170			
		I	760	CP-30, HPR	14.1	8.7	field emission
		II		CP-50, HPR	30.1	22.9 *	quench / (f.e)
K-3	200			Tum.-55, EP-250			
		I	760	HPR"	34.5	8.0	quench
		II		MSR, HPR"	32.2	9.8	quench
		III		CP-10, MSR	27.3	10.5	field emission
		IV		MSR, HPR"	30.8	12.4	quench
C-3	350			Tum.(-), EP-240			
		I	760	CP-15, HPR	33.0	6.2	quench
		II		CP-25, HPR"	31.3	—	field emission
		III		CP-30, HPR	26.4	16.8 *	field emission
		IV		CP-30, HPR	32.0	18.9 *	quench
		V	800	HPR	31.0	9.4	quench / (f.e)
		VI		no, (warm-up)	31.0	10.9	quench / (f.e)
		VII		no, (warm-up)	31.0	12.1	quench / (f.e)
M-1	100	(I, II)	1400	EP-200 (in the tests before removing the ceramic disk, [8])			
				Tum.-50, EP-200			
		III	760	CP-30, HPR	11.8	16.8	quench
		IV		CP-50, HPR	11.4	44.8 *	quench
K-1	200	(I, II)	1400	EP-110, CP-100 (in the tests before removing the ceramic disk, [8])			
				EP-110			
		III	760	CP-15, HPR	28.6	10.9	quench
				EP-110			
		IV	760	EP-20 H_2O_2, HPR	19.0	34.6 *	field emission
				Tum.-5, EP-10			
		V	800	CP-50, HPR	23 0	30.2 *	field emission
C-1	350	(I - VI)	1400	CP-250 (in the tests before removing the ceramic disk, [8])			
		VII		CP-50, HPR	31.5	9.8	quench
		VIII		CP-30, HPR	30.2	8.3	quench
		IX		no, (warm-up)	30 7	21.4 *	quench
		X		no, (warm-up)	28 7	9.7	quench
		XI		CP-10, HPR"	27.7	10.0	quench
		XII		CP-30, HPR	30.0	22.5 *	quench

[Tum./ tumbling (barrel polishing), EP / electro-polishing, CP / chemical polishing, HPR / high pressure water rinsing with ultrapure water (HPR"/ with pure water), * / installation of the temperature mapping system, f.e / field emission]